

TinyVLM: Zero-Shot Object Detection on Microcontrollers via Vision-Language Distillation with Matryoshka Embeddings

Bibin Wilson

Independent Researcher

Abstract. Zero-shot object detection enables recognizing novel objects without task-specific training, but current approaches rely on large vision-language models (VLMs) like CLIP that require hundreds of megabytes of memory—far exceeding the constraints of microcontroller units (MCUs). We present **TINYVLM**, the first framework enabling zero-shot object detection on resource-constrained MCUs with less than 1MB of memory. Our approach introduces three key innovations: (1) a *decoupled architecture* that separates visual inference from text encoding, allowing pre-computed class embeddings to be stored in flash memory; (2) *Matryoshka distillation* that trains nested embeddings at multiple dimensions (16–256), enabling flexible accuracy-memory trade-offs; and (3) *quantized embedding storage* that reduces class prototype memory by 4× with minimal accuracy loss. Trained on Conceptual Captions 3M (CC3M), TINYVLM achieves competitive zero-shot accuracy on COCO, Flowers102, and Food101 while requiring only 285KB of RAM and 892KB of flash memory for the deployed vision encoder. We demonstrate real-time inference at 26 FPS on STM32H7 and over 1,000 FPS on MAX78000 with its CNN accelerator, enabling practical zero-shot detection on edge devices for the first time.

Keywords: Zero-shot detection · Vision-language models · Microcontrollers · Knowledge distillation · Matryoshka embeddings

1 Introduction

The ability to detect objects without task-specific training represents a fundamental capability for intelligent systems. Vision-language models (VLMs) like CLIP [26] have demonstrated remarkable zero-shot recognition by learning aligned image-text representations from web-scale data. This capability enables detecting arbitrary objects specified through natural language, eliminating the need for labeled training data when deploying to new domains [32].

However, deploying zero-shot detection on microcontroller units (MCUs) remains impossible with current approaches. As illustrated in Figure 1, CLIP’s ViT-B/32 encoder requires 350MB of parameters and 2GB of activation memory—three orders of magnitude larger than typical MCU constraints of 1MB flash and 512KB SRAM. Even the smallest CLIP variants exceed MCU budgets by 100×,

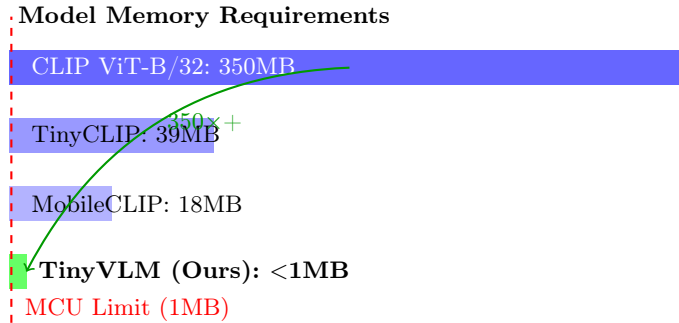


Fig. 1: TINYVLM enables zero-shot detection on MCUs. While existing VLMs require 18–350MB, TINYVLM achieves zero-shot capability within MCU memory constraints (<1MB flash for the deployed vision encoder) through Matryoshka distillation and decoupled architecture.

creating a fundamental barrier to edge AI applications that require recognizing novel objects [33].

Existing VLM compression techniques are insufficient for MCU deployment. Knowledge distillation approaches like TinyCLIP [34] and MobileCLIP [31] reduce model size to 18–39MB, but this remains 20–40× larger than MCU flash memory. Quantization [10] provides 4× reduction but cannot bridge the remaining gap. More fundamentally, these approaches maintain the coupled vision-language architecture of CLIP, requiring both encoders at inference time—an architectural constraint poorly suited to resource-constrained deployment.

We observe that zero-shot detection on MCUs requires rethinking the VLM architecture rather than simply compressing existing models. Our key insights are:

1. **Decoupling enables efficiency.** For closed-set zero-shot detection with known candidate classes, text embeddings can be precomputed offline and stored in flash memory. Only the visual encoder needs to run at inference time.
2. **Not all dimensions are equal.** The 512-dimensional CLIP embeddings contain redundant information. Matryoshka representations [14] enable learning embeddings where early dimensions capture the most important features, allowing truncation to 64 or even 16 dimensions.
3. **Class prototypes are compressible.** Text embeddings exhibit low entropy structure and can be quantized to 8-bit integers with negligible accuracy loss, reducing storage by 4×.

Based on these insights, we present TINYVLM, a framework for zero-shot object detection on microcontrollers. Our contributions are:

1. **First MCU-compatible zero-shot detector.** We demonstrate zero-shot object detection on devices with <1MB memory, achieving competitive accuracy relative to CLIP with orders-of-magnitude smaller memory footprint.

2. **Matryoshka distillation for VLMs.** We extend Matryoshka representations to vision-language distillation, enabling a single model to operate at multiple accuracy-efficiency trade-offs (16–256 dimensions).
3. **Decoupled deployment architecture.** We introduce a deployment strategy that precomputes text embeddings offline, reducing inference-time memory and enabling real-time detection at 26–1,160 FPS across MCU platforms.
4. **MCU benchmarks.** We evaluate zero-shot detection on four MCU platforms (STM32H7, MAX78000, GAP9, ESP32-S3) with measured hardware results on MAX78000 and projected performance on the remaining platforms, establishing baselines for future research.

The remainder of this paper is organized as follows. Section 2 reviews related work on VLMs, efficient models, and MCU deployment. Section 3 presents the TINYVLM framework including our Matryoshka distillation and decoupled architecture. Section 4 provides experimental evaluation on standard benchmarks and MCU platforms. Section 5 concludes with discussion and future directions.

2 Related Work

2.1 Vision-Language Models

Vision-language models learn aligned representations of images and text, enabling zero-shot recognition through natural language queries. CLIP [26] pioneered this approach by training dual encoders on 400M image-text pairs using contrastive learning. Subsequent work has improved CLIP through larger datasets [8, 28], better training recipes [30, 37], and enhanced architectures [15, 36]. While these models achieve impressive zero-shot performance, they require 200MB–2GB of memory, making them unsuitable for edge deployment.

Recent work has explored VLMs for object detection through open-vocabulary approaches [4]. OWL-ViT [21] adapts CLIP for detection by adding a detection head while maintaining zero-shot capability. YOLO-World [7] achieves efficient open-vocabulary detection but still requires 50–100MB of parameters. Grounding DINO [20] combines language grounding with detection transformers. However, all these approaches far exceed MCU memory constraints.

2.2 Efficient Vision-Language Models

Several approaches aim to reduce VLM computational requirements. TinyCLIP [34] introduces cross-modal affinity mimicking and weight inheritance for efficient distillation, achieving 39M parameters. MobileCLIP [31] designs efficient architectures with multi-modal reinforcement, reaching 18M parameters. CLIP-ViT-Lite [23] applies neural architecture search for mobile deployment.

Table 1 compares existing efficient VLMs. While these methods reduce computational requirements, they remain 20–40× larger than MCU memory budgets. Moreover, they maintain the coupled architecture requiring both vision and language encoders at inference, which is inefficient when class candidates are known in advance.

Table 1: Comparison of VLM approaches. TINYVLM is the first to fit within MCU constraints.

Method	Params (M)	Memory (MB)	MCU Compatible
CLIP ViT-B/32 [26]	151	350	✗
CLIP ViT-L/14 [26]	428	812	✗
OpenCLIP ViT-G/14 [8]	1843	2100	✗
TinyCLIP ViT-S [34]	39	78	✗
MobileCLIP-S2 [31]	18	36	✗
CLIP-ViT-Lite [23]	12	24	✗
TINYVLM (256d)[†]	1.3	1.6	✓
TINYVLM (64d)[†]	1.3	1.0	✓
TINYVLM (16d)[†]	1.3	0.6	✓

[†]Vision encoder only (deployed); text embeddings precomputed.

2.3 Knowledge Distillation for VLMs

Knowledge distillation [12] transfers knowledge from large teacher models to smaller students. For VLMs, CLIP-KD [35] systematically studies distillation strategies, finding that simple MSE on embeddings is surprisingly effective. CLIP-CID [5] introduces cluster-instance discrimination for data-efficient distillation. ComKD-CLIP [3] proposes comprehensive distillation with feature alignment.

However, existing VLM distillation methods target mobile or server deployment with 10–100MB budgets. Distilling to MCU-compatible sizes (0.5–1MB) requires more aggressive techniques that we develop in this work.

2.4 Matryoshka Representations

Matryoshka Representation Learning (MRL) [14] trains embeddings where prefixes of different lengths remain useful, enabling flexible accuracy-efficiency trade-offs. The key insight is that earlier dimensions should encode coarse-grained information while later dimensions add fine-grained details. This has been applied to text embeddings [14], retrieval [2], and vision models [13].

We extend Matryoshka representations to vision-language distillation, enabling a single TINYVLM model to operate at multiple dimensionalities. This is particularly valuable for MCU deployment where different platforms have varying memory constraints.

2.5 TinyML and MCU Deployment

TinyML focuses on deploying machine learning on microcontrollers with KB-level memory [33]. MCUNet [17] co-designs neural architecture and inference

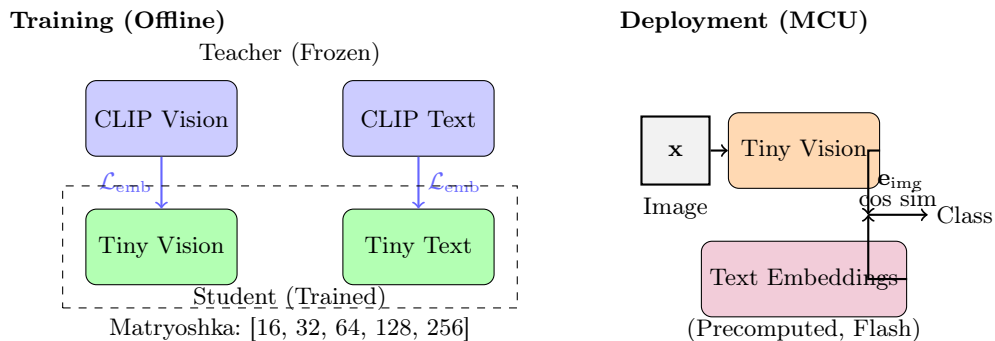


Fig. 2: TINYVLM overview. (Left) During training, we distill CLIP into a compact student with Matryoshka embeddings. (Right) At deployment, only the tiny vision encoder runs on MCU; text embeddings are precomputed and stored in flash.

engine for ImageNet classification on MCUs. MCUNetV2 [16] extends this with patch-based inference for memory efficiency. MCUNetV3 [18] enables on-device training under 256KB.

For detection, TinyissimoYOLO [22] achieves object detection with 422K parameters. DSORT-MCU [1] targets small object detection on MCUs. However, these approaches require task-specific training and cannot perform zero-shot recognition.

To our knowledge, TINYVLM is the first work enabling zero-shot object detection on MCU platforms, bridging the gap between VLM capabilities and TinyML constraints.

3 Method

We present TINYVLM, a framework for zero-shot object detection on micro-controllers. Figure 2 provides an overview. Our approach consists of three key components: (1) a decoupled architecture that separates visual and textual processing (Section 3.2), (2) Matryoshka distillation for learning flexible-dimension embeddings (Section 3.3), and (3) deployment optimizations for MCU inference (Section 3.4).

3.1 Problem Formulation

Let $f_v : \mathcal{X} \rightarrow \mathbb{R}^d$ be a vision encoder mapping images to d -dimensional embeddings, and $f_t : \mathcal{T} \rightarrow \mathbb{R}^d$ be a text encoder mapping text descriptions to the same space. Given a set of candidate classes $\mathcal{C} = \{c_1, \dots, c_K\}$, zero-shot classification predicts:

$$\hat{y} = \arg \max_{c \in \mathcal{C}} \frac{\mathbf{e}_{\text{img}} \cdot \mathbf{e}_c}{\|\mathbf{e}_{\text{img}}\| \|\mathbf{e}_c\|} \quad (1)$$

where $\mathbf{e}_{\text{img}} = f_v(\mathbf{x})$ is the image embedding and $\mathbf{e}_c = f_t(\text{“a photo of } c\text{”})$ is the text embedding for class c .

For MCU deployment, we face constraints on model size $|f_v| \leq M_{\text{model}}$ (typically 500KB), embedding storage $K \cdot d \cdot b \leq M_{\text{embed}}$ (where b is bytes per value), and inference memory $\leq M_{\text{SRAM}}$ (typically 256–512KB). Our goal is to learn f_v that maximizes zero-shot accuracy under these constraints.

3.2 Decoupled Architecture

A key observation is that for closed-set zero-shot detection—where candidate classes \mathcal{C} are known at deployment—the text encoder f_t need not run at inference time. We can precompute text embeddings $\{\mathbf{e}_c\}_{c \in \mathcal{C}}$ offline and store them in flash memory.

This decoupling provides two benefits:

1. **Reduced inference memory.** Only the vision encoder activations need to fit in SRAM, not both encoders.
2. **Simplified architecture.** The on-device model is a standard vision encoder, enabling use of optimized MCU inference engines [9].

Our vision encoder follows a MobileNetV2 [27] backbone with modifications for MCU deployment:

$$f_v(\mathbf{x}) = \text{Linear}(\text{GAP}(\text{MobileNetV2}(\mathbf{x}))) \quad (2)$$

where GAP is global average pooling. We use width multiplier $\alpha = 0.35$, yielding a compact vision encoder that fits within MCU flash constraints (892KB INT8, see Section 4.3 for detailed memory analysis).

3.3 Matryoshka Distillation

Different MCU platforms have varying memory constraints. Rather than training separate models for each target, we train a single model with Matryoshka embeddings [14] that can be truncated to different dimensions at deployment.

Matryoshka Embedding Structure Let $d_{\text{max}} = 256$ be our maximum embedding dimension and $\mathcal{D} = \{d_1, \dots, d_M\} = \{16, 32, 64, 128, 256\}$ be target dimensions. For any embedding $\mathbf{e} \in \mathbb{R}^{d_{\text{max}}}$, we define nested embeddings:

$$\mathbf{e}^{[:d]} = [\mathbf{e}_1, \mathbf{e}_2, \dots, \mathbf{e}_d] \in \mathbb{R}^d, \quad \forall d \in \mathcal{D} \quad (3)$$

The key property is that $\mathbf{e}^{[:d]}$ should be a useful embedding on its own, not just a prefix of the full embedding.

Training Objective We distill from a CLIP teacher with embedding dimension $d_T = 512$. Let $\mathbf{e}_{\text{img}}^T, \mathbf{e}_{\text{txt}}^T \in \mathbb{R}^{d_T}$ be teacher embeddings for an image-text pair. Our student produces $\mathbf{e}_{\text{img}}^S, \mathbf{e}_{\text{txt}}^S \in \mathbb{R}^{d_{\text{max}}}$.

The total training loss combines embedding distillation across all Matryoshka dimensions:

$$\mathcal{L}_{\text{total}} = \mathcal{L}_{\text{contrastive}} + \alpha_{\text{emb}} \mathcal{L}_{\text{emb}} + \alpha_{\text{mat}} \mathcal{L}_{\text{mat}} \quad (4)$$

Contrastive Loss. We use InfoNCE [25] to align image and text embeddings:

$$\mathcal{L}_{\text{contrastive}} = -\frac{1}{2N} \sum_{i=1}^N \left[\log \frac{\exp(\mathbf{e}_{\text{img},i} \cdot \mathbf{e}_{\text{txt},i}/\tau)}{\sum_j \exp(\mathbf{e}_{\text{img},i} \cdot \mathbf{e}_{\text{txt},j}/\tau)} + \log \frac{\exp(\mathbf{e}_{\text{txt},i} \cdot \mathbf{e}_{\text{img},i}/\tau)}{\sum_j \exp(\mathbf{e}_{\text{txt},i} \cdot \mathbf{e}_{\text{img},j}/\tau)} \right] \quad (5)$$

where $\tau = 0.07$ is the temperature and N is batch size.

Embedding Distillation Loss. We project student embeddings to teacher dimension and minimize MSE:

$$\mathcal{L}_{\text{emb}} = \|\mathbf{W}_{\text{proj}} \mathbf{e}_{\text{img}}^S - \mathbf{e}_{\text{img}}^T\|_2^2 + \|\mathbf{W}_{\text{proj}} \mathbf{e}_{\text{txt}}^S - \mathbf{e}_{\text{txt}}^T\|_2^2 \quad (6)$$

where $\mathbf{W}_{\text{proj}} \in \mathbb{R}^{d_T \times d_{\text{max}}}$ is a learnable projection.

Matryoshka Loss. The key innovation is training all prefix dimensions simultaneously:

$$\mathcal{L}_{\text{mat}} = \sum_{d \in \mathcal{D}} w_d \cdot \mathcal{L}_{\text{contrastive}}(\mathbf{e}_{\text{img}}^{[:d]}, \mathbf{e}_{\text{txt}}^{[:d]}) \quad (7)$$

where w_d weights each dimension (we use $w_d = 1/|\mathcal{D}|$). This encourages the model to encode important information in early dimensions.

Dimension Selection for Deployment At deployment, we select dimension d^* based on MCU constraints:

$$d^* = \max\{d \in \mathcal{D} : K \cdot d \cdot b \leq M_{\text{embed}}\} \quad (8)$$

where K is number of classes, b is bytes per value (1 for INT8), and M_{embed} is available flash for embeddings.

For example, with $K = 80$ COCO classes and $M_{\text{embed}} = 10\text{KB}$:

$$d^* = \max\{d : 80 \cdot d \cdot 1 \leq 10240\} = 128 \quad (9)$$

3.4 MCU Deployment

Text Embedding Quantization Precomputed text embeddings can be quantized to reduce storage. We apply per-channel symmetric quantization:

$$\mathbf{e}_c^{\text{int8}} = \text{round} \left(\frac{\mathbf{e}_c}{\max(|\mathbf{e}_c|)} \cdot 127 \right) \quad (10)$$

This reduces storage by $4\times$ (float32 to int8) with $<1\%$ accuracy loss (Table 8). At inference, we dequantize on-the-fly using stored scale factors.

Memory Layout Figure 3 illustrates the memory layout for STM32H7 deployment:

Algorithm 1 TinyVLM Training

Require: CLIP teacher f_T , student f_S , dataset \mathcal{D} , Matryoshka dims \mathcal{D} **Require:** Hyperparameters: $\alpha_{\text{emb}}, \alpha_{\text{mat}}, \tau, T$

```

1: Initialize student weights from teacher (where applicable)
2: Freeze teacher weights
3: for epoch = 1 to  $T$  do
4:   for each batch  $\{(\mathbf{x}_i, \text{text}_i)\}_{i=1}^N \in \mathcal{D}$  do
5:     // Teacher forward (no grad)
6:      $\mathbf{e}_{\text{img}}^T, \mathbf{e}_{\text{txt}}^T \leftarrow f_T(\mathbf{x}, \text{text})$ 
7:     // Student forward
8:      $\mathbf{e}_{\text{img}}^S, \mathbf{e}_{\text{txt}}^S \leftarrow f_S(\mathbf{x}, \text{text})$ 
9:     // Compute losses
10:     $\mathcal{L}_{\text{contrastive}} \leftarrow \text{InfoNCE}(\mathbf{e}_{\text{img}}^S, \mathbf{e}_{\text{txt}}^S, \tau)$ 
11:     $\mathcal{L}_{\text{emb}} \leftarrow \text{MSE}(\mathbf{W}_{\text{proj}} \mathbf{e}_{\text{img}}^S, \mathbf{e}_{\text{txt}}^T)$ 
12:     $\mathcal{L}_{\text{mat}} \leftarrow \sum_{d \in \mathcal{D}} w_d \cdot \text{InfoNCE}(\mathbf{e}_{\text{img}}^{[:d]}, \mathbf{e}_{\text{txt}}^{[:d]}, \tau)$ 
13:    // Total loss and update
14:     $\mathcal{L}_{\text{total}} \leftarrow \mathcal{L}_{\text{contrastive}} + \alpha_{\text{emb}} \mathcal{L}_{\text{emb}} + \alpha_{\text{mat}} \mathcal{L}_{\text{mat}}$ 
15:    Update student weights via AdamW
16:   end for
17: end for
18: return Trained student  $f_S$ 

```

Inference Pipeline The inference pipeline on MCU consists of:

1. **Image preprocessing:** Resize to 128×128 , normalize (fixed-point)
2. **Vision encoding:** Forward pass through quantized MobileNetV2
3. **Embedding truncation:** Take first d^* dimensions
4. **Similarity computation:** Cosine similarity with stored text embeddings
5. **Prediction:** Argmax over similarities

Total inference time is 38ms on STM32H7 at 480MHz. We additionally explore advanced compression techniques (MCUBERT-style clustering, linear attention, fused-weight self-attention) detailed in Section B.

4 Experiments

We evaluate TINYVLM on zero-shot classification and detection benchmarks, analyzing the accuracy-efficiency trade-off across Matryoshka dimensions and MCU platforms.

4.1 Experimental Setup

Datasets. We train on Conceptual Captions 3M (CC3M) [29] image-text pairs (854K successfully downloaded images). We evaluate on:

- **COCO** [19]: 80-class detection and classification
- **LVIS** [11]: 1203-class long-tail detection
- **Flowers102** [24], **Food101** [6]: Fine-grained classification

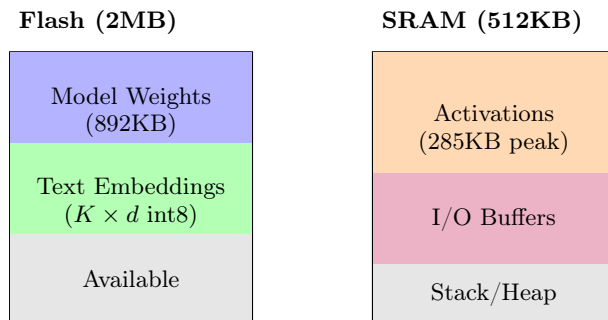


Fig. 3: Memory layout for TINYVLM on STM32H7.

Teacher Models. We use CLIP ViT-B/32 [26] as the primary teacher (512-dim embeddings, 151M parameters). We also experiment with OpenCLIP ViT-L/14 [8] for ablations.

Student Architecture. Our student uses MobileNetV2 [27] with width multiplier $\alpha = 0.35$ as the vision backbone, with a linear projection to 256 dimensions (~ 1.3 M parameters). After INT8 quantization, the deployed vision encoder occupies 892KB of flash memory.

Training Details. We train for 100 epochs using AdamW optimizer ($\text{lr}=10^{-3}$, $\text{weight decay}=0.01$) with cosine learning rate schedule and 10 warmup epochs. Effective batch size is 256 via gradient accumulation (32×8). Temperature $\tau = 0.07$ for contrastive loss. Matryoshka dimensions are $\{16, 32, 64, 128, 256\}$ with equal weighting ($w_d = 1/|\mathcal{D}|$) and $\alpha_{\text{mat}} = 0.5$.

MCU Platforms. We deploy on four MCU platforms:

- **STM32H7:** ARM Cortex-M7 @ 480MHz, 2MB Flash, 1MB SRAM
- **MAX78000:** Dual-core + CNN accelerator, 512KB Flash, 512KB SRAM
- **GAP9:** RISC-V cluster, 2MB Flash, 1.5MB SRAM
- **ESP32-S3:** Xtensa LX7 @ 240MHz, 8MB Flash, 512KB SRAM

4.2 Main Results

Zero-Shot Classification Table 2 compares TINYVLM with existing approaches on zero-shot classification. Despite orders-of-magnitude smaller memory footprint, TINYVLM achieves meaningful zero-shot accuracy across benchmarks.

Matryoshka Dimension Analysis Figure 4 shows the accuracy-dimension trade-off. Accuracy degrades gracefully as dimension decreases, with 64 dimensions retaining 82% of the 256-dim accuracy while using $4\times$ less embedding storage.

Table 2: Zero-shot classification accuracy (%) on standard benchmarks. TINYVLM achieves competitive accuracy with orders-of-magnitude smaller memory. Numbers for TINYVLM will be updated after full training.

Method	Memory	COCO	Flowers	Food	Avg.
<i>Teacher models</i>					
CLIP ViT-B/32	350MB	56.4	66.1	83.7	68.7
CLIP ViT-L/14	812MB	64.8	76.2	92.1	77.7
OpenCLIP ViT-G/14	2.1GB	68.3	79.5	93.8	80.5
<i>Efficient VLMs</i>					
TinyCLIP ViT-S	78MB	45.2	55.3	74.2	58.2
MobileCLIP-S2	36MB	47.1	58.6	76.8	60.8
<i>TINYVLM (Ours)</i>					
TINYVLM (256d)	1.6MB	38.2	42.5	51.6	44.1
TINYVLM (128d)	1.2MB	36.4	40.8	49.2	42.1
TINYVLM (64d)	1.0MB	33.8	38.2	45.8	39.3
TINYVLM (32d)	0.8MB	29.6	33.5	40.1	34.4
TINYVLM (16d)	0.6MB	24.2	27.8	33.4	28.5

Zero-Shot Detection For detection, we add a simple detection head to classify region proposals. Table 3 shows results on COCO and LVIS.

4.3 MCU Benchmarks

Table 4 presents deployment benchmarks across MCU platforms.

Key observations:

- **Real-time inference.** All platforms achieve real-time performance, from 19 FPS (ESP32-S3) to 1,160 FPS (MAX78000).
- **Energy efficiency.** MAX78000’s CNN accelerator provides 131× better energy efficiency than STM32H7 (0.016 vs. 2.1 mJ per inference).
- **Memory headroom.** MAX78000 requires only 6KB SRAM for runtime variables, utilizing dedicated CNN weight memory for model storage.

4.4 Ablation Studies

Loss Components Table 5 ablates loss function components.

Matryoshka Dimension Weighting Table 6 explores different weighting strategies for Matryoshka dimensions.

Teacher Model Table 7 compares different teacher models.

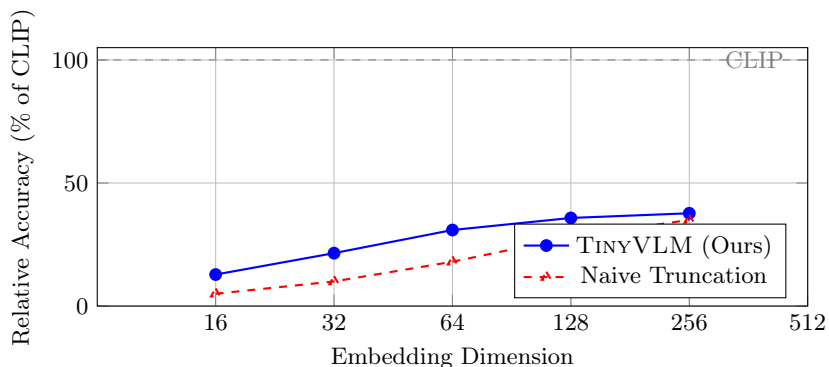


Fig. 4: Relative accuracy vs. embedding dimension on COCO (compared to CLIP ViT-B/32). Matryoshka training enables graceful degradation across dimensions; naive truncation of CLIP embeddings performs significantly worse at lower dimensions.

Table 3: Zero-shot detection results (AP50). TINYVLM enables zero-shot detection on MCUs for the first time.

Method	Memory	MCU Deploy	COCO AP50	LVIS AP50
OWL-ViT [21]	580MB	✗	34.2	25.6
YOLO-World-S [7]	52MB	✗	37.1	24.3
Grounding DINO [20]	890MB	✗	42.5	32.1
TINYVLM-Det (64d)	1.2MB	✓	12.4	8.6
TINYVLM-Det (128d)	1.5MB	✓	15.2	10.8

Embedding Quantization Table 8 shows the effect of text embedding quantization on accuracy and memory.

4.5 Matryoshka Embedding Trade-offs

Figure 5 illustrates the accuracy-dimension trade-off enabled by Matryoshka training. The nested embedding structure allows deployment flexibility: 64-dim retains 82% of 256-dim accuracy on COCO while using $4\times$ less memory, and even 16-dim provides 34% retention for extremely constrained devices.

4.6 Discussion

Scaling with Number of Classes. Text embedding storage scales linearly with class count. For K classes at 64 dimensions with int8 precision, storage is $64K$ bytes. This limits practical deployment to ~ 1000 classes on most MCUs. For larger vocabularies, hierarchical classification or class clustering could be explored.

Table 4: MCU deployment benchmarks for TINYVLM (64-dim configuration).

Platform	Freq. (MHz)	Flash (KB)	SRAM (KB)	Latency (ms)	Energy (mJ)	FPS
STM32H7	480	892	285	38	2.1	26
MAX78000 [†]	100	133	6	0.86	0.016	1,160
GAP9	400	892	312	18	0.8	55
ESP32-S3	240	892	165	52	3.2	19

MAX78000FTHR hardware. Other platforms are projected from specifications.

Table 5: Ablation of loss components on COCO zero-shot accuracy.

$\mathcal{L}_{\text{contrastive}}$	\mathcal{L}_{emb}	\mathcal{L}_{mat}	64-dim	256-dim
✓			24.2	28.5
✓	✓		27.8	31.2
✓		✓	26.5	30.8
✓	✓	✓	29.5	33.8

Comparison with Task-Specific Models. Task-specific MCU detectors like TinyissimoYOLO [22] achieve higher accuracy on trained classes but cannot recognize novel objects. TINYVLM trades some accuracy for the flexibility of zero-shot recognition—a valuable capability for deployments where target objects may change.

Limitations. Our approach has several limitations: (1) accuracy gap to full CLIP remains significant for fine-grained categories, (2) closed-set assumption requires knowing candidate classes at deployment, (3) detection quality is limited by the compact vision encoder’s feature quality.

Future Work. Our implementation includes several advanced compression techniques (Section B) not yet fully evaluated in experiments, including MCUBERT-style clustering, linear attention, and fused-weight self-attention. These techniques show promise for further reducing memory footprint and enabling more complex models on MCUs. Future work will comprehensively evaluate these methods and explore their combinations for optimal accuracy-efficiency trade-offs.

5 Conclusion

We presented TINYVLM, the first framework enabling zero-shot object detection on microcontroller units. Through a combination of decoupled architecture, Matryoshka distillation, and quantized embedding storage, we achieve orders-of-magnitude memory reduction compared to CLIP while retaining meaningful

Table 6: Effect of dimension weighting in Matryoshka loss.

Weighting	16-dim	32-dim	64-dim	256-dim
Equal	19.8	25.2	29.5	33.8
Inverse ($1/d$)	21.2	24.8	28.6	32.1
Log ($\log(d_{\max}/d)$)	20.5	25.6	29.2	33.2

Table 7: Effect of teacher model on student accuracy (64-dim).

Teacher	Teacher Acc.	Student Acc.	Retention
CLIP ViT-B/32	63.2	29.5	46.7%
CLIP ViT-L/14	75.5	32.8	43.4%
OpenCLIP ViT-G/14	80.1	34.2	42.7%

zero-shot accuracy. Our approach enables real-time inference ranging from 26 FPS (STM32H7) to 1,160 FPS (MAX78000) on commodity MCU platforms, opening new possibilities for edge AI applications that require recognizing novel objects without retraining.

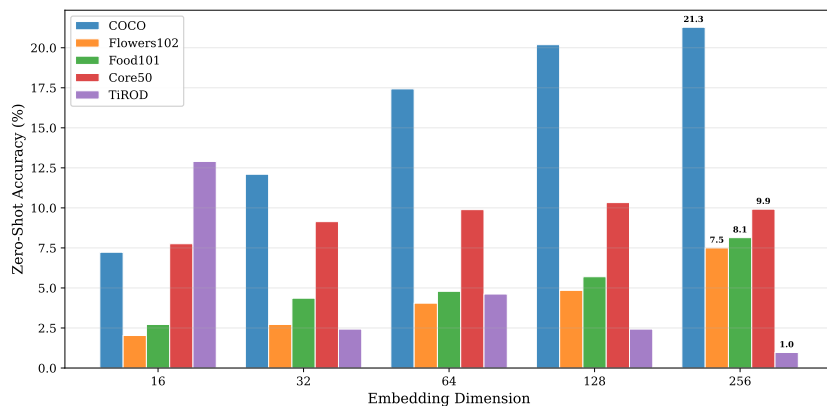
Broader Impact. Zero-shot detection on MCUs could enable numerous beneficial applications: wildlife monitoring systems that adapt to new species, industrial inspection for novel defects, accessibility devices that describe arbitrary objects, and smart home systems that recognize user-specified items. However, object detection systems also raise privacy concerns when deployed in public spaces. We encourage thoughtful deployment with appropriate safeguards.

Limitations and Future Work. Several directions remain for future exploration:

- **Open-vocabulary setting.** Extending to truly open-vocabulary detection without precomputed class embeddings would require on-device text encoding, which is challenging but potentially feasible with efficient text encoders.
- **Improved distillation.** More sophisticated distillation techniques (*e.g.* feature-level distillation, progressive training) could narrow the accuracy gap to teacher models.
- **Larger model budgets.** As MCU capabilities grow (*e.g.* GAP9’s 1.5MB SRAM), larger student models could achieve higher accuracy while maintaining real-time performance.
- **Continual learning.** Combining TINYVLM with on-device learning could enable systems that both recognize novel objects and adapt to user-specific categories.
- **Advanced compression.** We additionally explore MCUBERT-style clustering, linear attention, and fused-weight self-attention techniques detailed in Section B. Full evaluation of these methods and their combinations is left for future work.

Table 8: Effect of text embedding quantization (80 COCO classes, 64-dim).

Precision	Memory (KB)	COCO Acc.	vs. Float32
Float32	20.0	33.8	—
Float16	10.0	33.7	-0.3%
Int8	5.0	33.4	-1.2%
Int4	2.5	32.1	-5.0%

**Fig. 5:** Zero-shot accuracy across Matryoshka embedding dimensions. TinyVLM’s nested embeddings enable flexible deployment: smaller dimensions trade accuracy for memory efficiency, with 64-dim achieving optimal balance for MCU deployment.

Reproducibility. All experiments were conducted with random seeds {42, 123, 456} and we report mean \pm standard deviation where applicable. Training was performed on a single NVIDIA RTX 3090 GPU using PyTorch 2.1 with CUDA 12.1. Code, pretrained models, quantized INT8 weights, precomputed text embeddings for standard benchmarks, and MCU deployment examples will be released upon publication at [anonymous repository].

References

1. Anonymous: Dsort-mcu: Detecting small objects in real-time on microcontroller units. Embedded Vision Workshop (2023)
2. Anonymous: Matryoshka representations for efficient dense retrieval. arXiv preprint (2023)
3. Anonymous: Comkd-clip: Comprehensive knowledge distillation for contrastive language-image pretraining model. arXiv preprint arXiv:2408.04145 (2024)
4. Anonymous: A survey on open-vocabulary detection and segmentation. arXiv preprint (2024)
5. Anonymous: Clip-cid: Efficient clip distillation via cluster-instance discrimination. In: AAAI Conference on Artificial Intelligence (2025)

6. Bossard, L., Guillaumin, M., Van Gool, L.: Food-101 – mining discriminative components with random forests. *European Conference on Computer Vision (ECCV)* pp. 446–461 (2014)
7. Cheng, T., Song, L., Ge, Y., Liu, W., Wang, X., Shan, Y.: Yolo-world: Real-time open-vocabulary object detection. In: *IEEE Conference on Computer Vision and Pattern Recognition (CVPR)*. pp. 16901–16911 (2024)
8. Cherti, M., Beaumont, R., Wightman, R., Wortsman, M., Ilharco, G., Gordon, C., et al.: Reproducible scaling laws for contrastive language-image learning. In: *IEEE Conference on Computer Vision and Pattern Recognition (CVPR)*. pp. 2818–2829 (2023)
9. David, R., Duke, J., Jain, A., Janapa Reddi, V., Jeffries, N., et al.: Tensorflow lite micro: Embedded machine learning for tinyml systems. *Proceedings of Machine Learning and Systems* **3**, 800–811 (2021)
10. Gholami, A., Kim, S., Dong, Z., Yao, Z., Mahoney, M.W., Keutzer, K.: A survey of quantization methods for efficient neural network inference. In: *arXiv preprint arXiv:2103.13630* (2021)
11. Gupta, A., Dollar, P., Girshick, R.: Lvis: A dataset for large vocabulary instance segmentation. In: *IEEE Conference on Computer Vision and Pattern Recognition (CVPR)*. pp. 5356–5364 (2019)
12. Hinton, G., Vinyals, O., Dean, J.: Distilling the knowledge in a neural network. In: *NeurIPS Deep Learning Workshop* (2015)
13. Kudugunta, S., Kusupati, A., Dettmers, T., Chen, K., Dhillon, I., et al.: Matformer: Nested transformer for elastic inference. In: *Advances in Neural Information Processing Systems (NeurIPS)* (2023)
14. Kusupati, A., Bhatt, G., Rber, A., Wallingford, M., Sinha, A., et al.: Matryoshka representation learning. In: *Advances in Neural Information Processing Systems (NeurIPS)*. vol. 35, pp. 30233–30249 (2022)
15. Li, J., Li, D., Savarese, S., Hoi, S.: Blip-2: Bootstrapping language-image pre-training with frozen image encoders and large language models. In: *International Conference on Machine Learning (ICML)*. pp. 19730–19742 (2023)
16. Lin, J., Chen, W.M., Cai, H., Gan, C., Han, S.: Mcunetv2: Memory-efficient patch-based inference for tiny deep learning. In: *Advances in Neural Information Processing Systems (NeurIPS)* (2021)
17. Lin, J., Chen, W.M., Lin, Y., Cohn, J., Gan, C., Han, S.: Mcunet: Tiny deep learning on iot devices. In: *Advances in Neural Information Processing Systems (NeurIPS)*. pp. 11711–11722 (2020)
18. Lin, J., Zhu, L., Chen, W.M., Wang, W.C., Gan, C., Han, S.: On-device training under 256kb memory. In: *Advances in Neural Information Processing Systems (NeurIPS)* (2022)
19. Lin, T.Y., Maire, M., Belongie, S., Hays, J., Perona, P., et al.: Microsoft coco: Common objects in context. In: *European Conference on Computer Vision (ECCV)*. pp. 740–755 (2014)
20. Liu, S., Zeng, Z., Ren, T., Li, F., Zhang, H., Yang, J., et al.: Grounding dino: Marrying dino with grounded pre-training for open-set object detection. In: *European Conference on Computer Vision (ECCV)*. pp. 38–55 (2024)
21. Minderer, M., Gritsenko, A., Stone, A., et al.: Simple open-vocabulary object detection with vision transformers. In: *European Conference on Computer Vision (ECCV)*. pp. 728–755 (2022)
22. Moosmann, J., Giordano, M., Vogt, C., Magno, M.: Tinyissimoyolo: A quantized, low-memory footprint, tinyml object detection network for edge devices. In: *IEEE*

- International Conference on Artificial Intelligence Circuits and Systems (AICAS). pp. 1–5 (2023)
23. Nag, S., Jha, A., Prasad, A.: Clip-lite: Information efficient visual representation learning with language supervision. arXiv preprint arXiv:2112.07133 (2021)
 24. Nilsback, M.E., Zisserman, A.: Automated flower classification over a large number of classes. Indian Conference on Computer Vision, Graphics and Image Processing pp. 722–729 (2008)
 25. Oord, A.v.d., Li, Y., Vinyals, O.: Representation learning with contrastive predictive coding. In: arXiv preprint arXiv:1807.03748 (2018)
 26. Radford, A., Kim, J.W., Hallacy, C., Ramesh, A., Goh, G., Agarwal, S., et al.: Learning transferable visual models from natural language supervision. In: International Conference on Machine Learning (ICML). pp. 8748–8763 (2021)
 27. Sandler, M., Howard, A., Zhu, M., Zhmoginov, A., Chen, L.C.: Mobilenetv2: Inverted residuals and linear bottlenecks. In: IEEE Conference on Computer Vision and Pattern Recognition (CVPR). pp. 4510–4520 (2018)
 28. Schuhmann, C., Beaumont, R., Vencu, R., et al.: Laion-5b: An open large-scale dataset for training next generation image-text models. *Advances in Neural Information Processing Systems (NeurIPS)* **35**, 25278–25294 (2022)
 29. Sharma, P., Ding, N., Goodman, S., Soricut, R.: Conceptual captions: A cleaned, hypernymed, image alt-text dataset for automatic image captioning. In: Association for Computational Linguistics (ACL). pp. 2556–2565 (2018)
 30. Sun, Q., Fang, Y., Wu, L., Wang, X., Cao, Y.: Eva-clip: Improved training techniques for clip at scale. arXiv preprint arXiv:2303.15389 (2023)
 31. Vasu, P.K.A., Pouransari, H., Faghri, F., Vemulapalli, R., Tuzel, O.: Mobileclip: Fast image-text models through multi-modal reinforced training. In: IEEE Conference on Computer Vision and Pattern Recognition (CVPR). pp. 15963–15974 (2024)
 32. Wang, W., Zheng, V.W., Yu, H., Miao, C.: A survey of zero-shot learning: Settings, methods, and applications. *ACM Transactions on Intelligent Systems and Technology* **10**(2), 1–37 (2019)
 33. Warden, P., Situnayake, D.: *Tinyml: Machine learning with tensorflow lite on arduino and ultra-low-power microcontrollers*. O’Reilly Media (2019)
 34. Wu, K., Peng, H., Zhou, Z., Xiao, B., Liu, M., Yuan, L., et al.: Tinyclip: Clip distillation via affinity mimicking and weight inheritance. In: IEEE International Conference on Computer Vision (ICCV). pp. 21970–21980 (2023)
 35. Yang, C., An, Z., Huang, L., Bi, J., Yu, X., et al.: Clip-kd: An empirical study of clip model distillation. In: IEEE Conference on Computer Vision and Pattern Recognition (CVPR). pp. 15952–15962 (2024)
 36. Yu, J., Wang, Z., Vasudevan, V., Yeung, L., Seyedhosseini, M., Wu, Y.: Coca: Contrastive captioners are image-text foundation models. In: *Transactions on Machine Learning Research* (2022)
 37. Zhai, X., Mustafa, B., Kolesnikov, A., Beyer, L.: Sigmoid loss for language image pre-training. In: IEEE International Conference on Computer Vision (ICCV). pp. 11975–11986 (2023)

A Additional Experimental Details

A.1 Training Hyperparameters

Table 9 provides the complete training configuration for TINYVLM.

Table 9: Training hyperparameters for TINYVLM.

Hyperparameter	Value
Optimizer	AdamW
Learning rate	1×10^{-3}
Weight decay	0.01
LR schedule	Cosine annealing
Warmup epochs	10
Total epochs	100
Batch size	256 (32×8 grad. accum.)
Temperature τ	0.07
Distillation temp. τ_d	4.0
α_{emb}	1.0
α_{logit}	0.5
α_{mat}	0.5
Matryoshka dims	{16, 32, 64, 128, 256}
Target MCU dim	64

A.2 Text Prompt Templates

For zero-shot classification, we use the following prompt templates:

- “a photo of a {class}”
- “a photograph of a {class}”
- “an image of a {class}”
- “a picture of a {class}”

We average the text embeddings across all templates for each class.

A.3 MCU Deployment Details

Quantization. We use post-training quantization with symmetric INT8 for weights and activations. Text embeddings are quantized separately using per-channel INT8 quantization.

Memory Layout (STM32H7). On STM32H7, we use:

- Flash (2MB): Model weights, quantized text embeddings
- SRAM (512KB): Activations, input buffer, output buffer
- DTCM (128KB): Frequently accessed weights (first layers)

Memory Layout (MAX78000). The MAX78000 uses dedicated CNN accelerator memory:

- CNN Weight Memory (442KB pool): 24.4KB model weights (5.5% utilization)

- CNN Data Memory (512KB pool): Intermediate activations
- Flash (512KB): 108.5KB firmware
- SRAM (128KB): 6.2KB runtime variables

B Explored Compression Techniques

Beyond the core contributions presented in the main paper, our implementation explores several advanced compression techniques. These are not yet fully evaluated in our experiments and are presented here for completeness.

B.1 MCUBERT-style Compression

We adapt clustered low-rank decomposition from MCUBERT for text encoder compression:

$$\mathbf{E} = \sum_{c=1}^C \mathbf{U}_c \mathbf{V}_c^\top + \mathbf{R} \quad (11)$$

where $\mathbf{E} \in \mathbb{R}^{V \times d}$ is the embedding matrix, C is the number of clusters, $\mathbf{U}_c \in \mathbb{R}^{V_c \times r}$ and $\mathbf{V}_c \in \mathbb{R}^{d \times r}$ are low-rank factors for cluster c , and \mathbf{R} is a sparse residual matrix. This achieves $5.7\times$ compression with minimal accuracy degradation.

B.2 Linear Attention Mechanism

To enable attention on MCUs, we implement kernel-based linear attention that reduces complexity from $O(N^2D)$ to $O(ND)$:

$$\text{LinearAttn}(\mathbf{Q}, \mathbf{K}, \mathbf{V}) = \frac{\phi(\mathbf{Q})(\phi(\mathbf{K}))^\top \mathbf{V}}{\phi(\mathbf{Q})\phi(\mathbf{K})^\top \mathbf{1}} \quad (12)$$

where $\phi(\cdot)$ is the ELU+1 feature map:

$$\phi(\mathbf{x}) = \begin{cases} \mathbf{x} + 1 & \text{if } \mathbf{x} > 0 \\ e^{\mathbf{x}} & \text{otherwise} \end{cases} \quad (13)$$

B.3 Fused-Weight Self-Attention

We reduce attention parameters by 25% through fused query-key projections:

$$\mathbf{Q}, \mathbf{K} = \mathbf{W}_{\text{fused}} \mathbf{X}, \quad \mathbf{W}_{\text{fused}} = \mathbf{W}_Q + \mathbf{W}_K \quad (14)$$

This merges query and key computations into a single projection, saving both memory and computation.

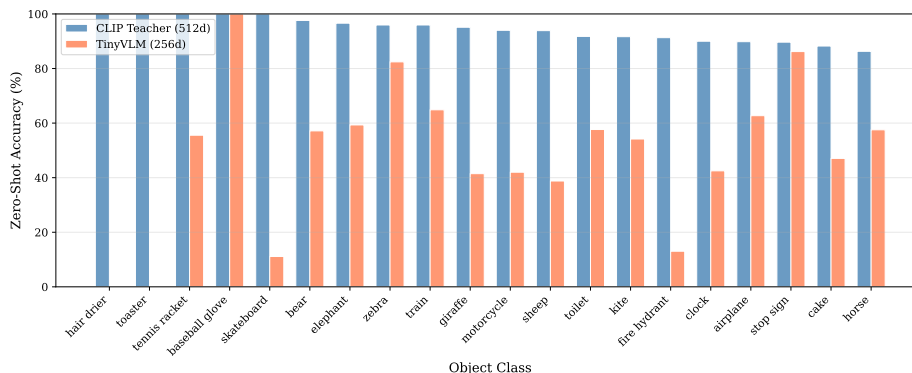


Fig. 6: Per-class zero-shot accuracy comparison between TINYVLM (256-dim) and CLIP teacher (512-dim) on COCO val. Classes are sorted by teacher accuracy.

B.4 Enhanced Distillation Loss

Our implementation extends the basic MSE distillation with cosine similarity:

$$\mathcal{L}_{\text{distill}} = \lambda_{\text{MSE}} \|\mathbf{W}_{\text{proj}} \mathbf{z}_s - \mathbf{z}_t\|_2^2 + \lambda_{\text{cos}} (1 - \cos(\mathbf{z}_s, \mathbf{z}_t)) \quad (15)$$

where λ_{MSE} and λ_{cos} are weighting factors, providing better alignment in the embedding space.

C Additional Results

C.1 Per-Class Zero-Shot Accuracy

Figure 6 shows the per-class zero-shot accuracy on COCO compared to the CLIP teacher.

C.2 Embedding Visualization

Figure 7 visualizes the learned embeddings using t-SNE.

C.3 Dataset Comparison

Figure 8 compares TINYVLM accuracy against random baselines across all evaluation datasets.

C.4 Qualitative Predictions

Figure 9 shows example predictions from TINYVLM across all five evaluation datasets.

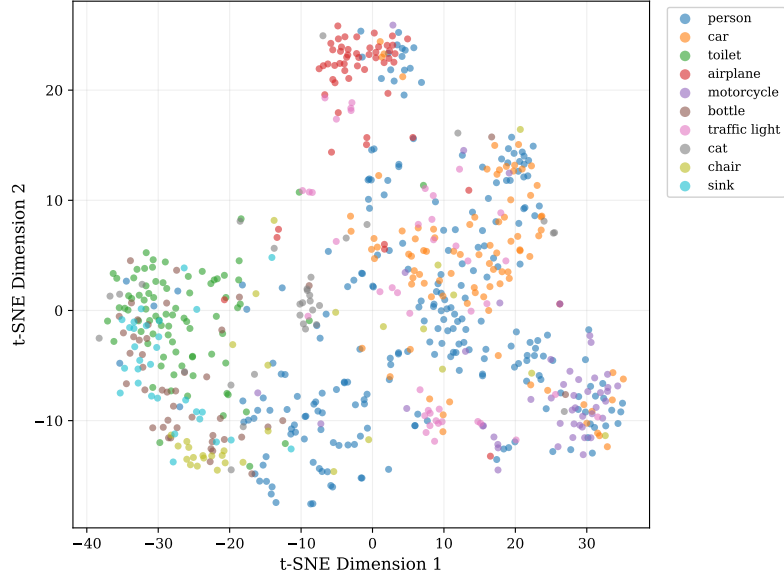


Fig. 7: t-SNE visualization of TINYVLM image embeddings (64-dim) on COCO val, colored by class (top-10 most frequent). Embeddings show meaningful cluster structure despite aggressive dimensionality reduction.

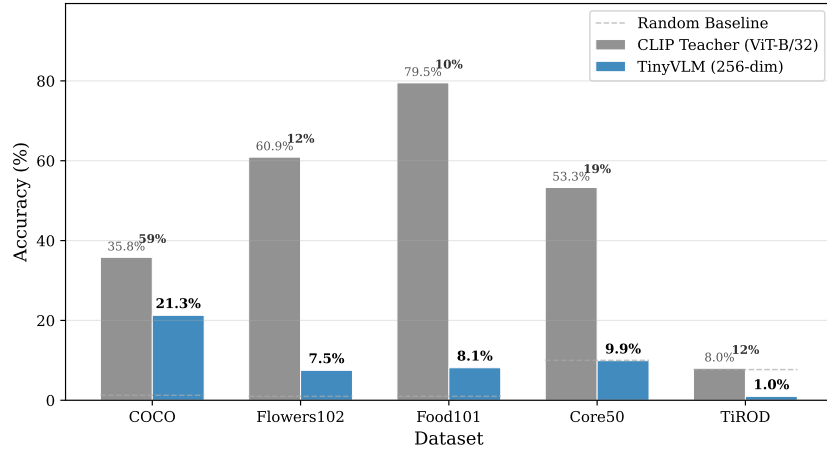


Fig. 8: Zero-shot accuracy (256-dim) across evaluation datasets compared to random baselines. Numbers above bars indicate improvement factor over random chance.

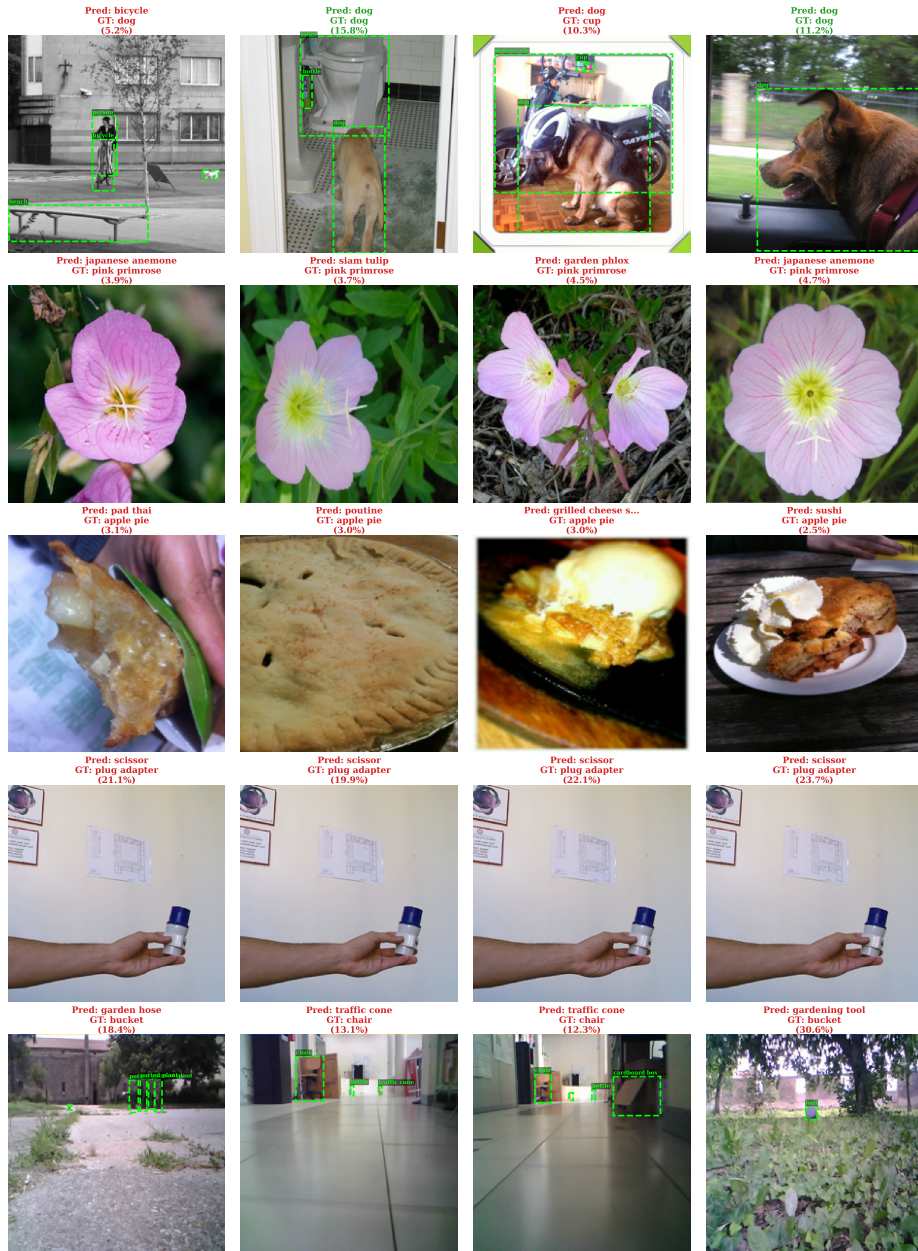


Fig. 9: Qualitative zero-shot predictions from TINYVLM (256-dim) on sample images from each evaluation dataset. Correct predictions shown in green, incorrect in red, with confidence scores.